Article

Not peer-reviewed version

Parametric Design Investigation and Mechanical Performance of Laser-Cut Kerf Bending in Plywood Sheets

Evangelos Grasos , Georgios Ntalos , Konstantinos Ninikas *

Posted Date: 18 March 2026

doi: 10.20944/preprints202603.1396.v1

Keywords: kerf bending; laser cutting; flexible wood; ergonomic seating; furniture design; digital fabrication; parametric design; material flexibility

 doi:10.20944/preprints202603.1396.v1

Article

Parametric Design Investigation and Mechanical Performance of Laser-Cut Kerf Bending in Plywood Sheets

Evangelos Grasos, Georgios Ntalos and Konstantinos Ninikas *

Department of Forestry, Wood Science and Design, University of Thessaly, GR-431 00 Karditsa, Greece
* Correspondence: kninikas@uth.gr; Tel.: +302441064722

Abstract

Kerf bending, a technique for curving material through repeated cuts, has evolved into a powerful tool in design and construction. Following experimental methodology, aiming at the design and construction of flexible and functional surfaces at real scale, this paper presents a creative Kerf Bending technique using a laser-cutting CNC machine. This research reviews the relevant techniques related to geometries, bending methods, and parameters that affect the behaviour of the material, wood. A systematic experimental process was undertaken, involving several birch plywood test specimens, on which different patterns were cut. The mechanical properties of the samples are tested to accurately record the performance under deformation, elasticity, and flexibility of each specimen. Comparative analysis showed that kerf geometry is the primary factor influencing the bending performance of plywood panels, having a greater impact than thickness or material removal percentage. Thinner specimens consistently demonstrated improved curvature capacity and higher load resistance, indicating more efficient stress distribution during deformation. Flexibility and strength were not directly proportional to the amount of removed material; instead, geometrically optimised layouts achieved favourable deformation while retaining mechanical integrity, whereas excessive removal reduced structural performance. The findings confirm that carefully designed kerf patterns can balance flexibility, strength, and aesthetic quality, supporting their use in structurally functional bent plywood components.

Keywords: kerf bending; laser cutting; flexible wood; ergonomic seating; furniture design; digital fabrication; parametric design; material flexibility

1. Introduction

Wood's strength, beauty, and workability have made it a basic material for ages in furniture, design, and construction. However, its natural rigidity and anisotropy limit its application in contexts requiring curvature or flexibility. Conventional techniques such as steam bending and lamination are labour-intensive, material-demanding, and constrained by the physical characteristics of specific wood species [1]. These challenges have prompted researchers and designers to explore alternative fabrication methods that enhance flexibility without compromising the inherent properties of wood [2].

Kerf bending, a technique in which a series of partial cuts are introduced into a rigid material, allows for controlled deformation by reducing stiffness along the cut direction. When applied to wood, kerf patterns create hinge-like zones that enable the material to bend while maintaining overall continuity [3]. The geometry, spacing, and depth of kerf cuts significantly influence the achievable curvature, structural integrity, and aesthetic outcomes [4].

 doi:10.20944/preprints202603.1396.v1

Recent advancements in digital fabrication technologies have made kerf bending more accessible to architects and designers, presenting opportunities to engineer materials with intensified precision [2,5]. Among these technologies, laser cutting is particularly noteworthy due to its high accuracy and repeatability in generating intricate kerf patterns. Unlike traditional, manual or CNC router methods, laser cutters excel at rapid prototyping, facilitating the creation of complex kerf geometries with minimal tool wear [6,7]. Research indicates that the optimisation of laser cutting parameters directly affects kerf quality, which subsequently influences the edge finish and coherence of the cuts [8–12].

Previous studies have demonstrated the potential of kerf bending for developing flexible surfaces, architectural installations, and experimental design objects [13,14]. However, systematic exploration of its functional application in ergonomic seating remains limited.

Seating design requires a balance between comfort, structural stability, and aesthetic appeal. Ergonomic chairs often rely on materials that adapt to the user's body while distributing load effectively [15]. The integration of kerf bending into seat construction provides a novel approach to achieving localised flexibility in otherwise rigid wooden components. This method enables the creation of forms that conform to ergonomic requirements without the need for additional upholstery or complex joinery [16].

Kerf bending offers a versatile method for inducing controlled curvature within planar materials. By introducing patterned separations in the form of kerf arrays, it enables adjacent regions to bend cohesively along defined boundaries. These kerfs act as flexible joints, giving rise to hinge-like behaviour that allows flat materials to assume complex, curved, or folded geometries.

Laser fabrication provides an exceptional level of precision in defining kerf geometry. The ability to finely control widths, spacings, and angles enables predictable deformation and consistent mechanical response. Consequently, laser kerfing extends the potential of traditional bending methods, ensuring repeatable structural performance and expanding design freedom for architectural and furniture applications.

Kerf bending represents a modern approach to wood deformation, relying on a network of fine, shallow cuts to locally reduce stiffness while maintaining material continuity. Each kerf functions as a mechanical hinge that governs bending direction and curvature.

Laser cutting is particularly effective for producing such precise arrays. It offers a high degree of accuracy and reproducibility in defining kerf geometry—parameters that ultimately dictate the bending behaviour and flexibility of the surface. Despite a growing body of literature on kerf performance, limited research has explored laser-based kerf creation for industrial-scale flexible wood applications. This study aims to bridge that gap through systematic experimentation and prototyping.

Although kerf bending appears contemporary, it is rooted in traditional wood-forming techniques such as kerf lamination—historically employed to create curved surfaces [17–23]. Over time, bending techniques have evolved alongside laminated and composite materials, including honeycomb and sandwich structures.

In furniture design, laser-crafted kerf arrays offer a promising path for achieving adaptable and ergonomic seating surfaces. Since the human body is dynamic and continuously adjusts posture, seating must respond flexibly to these micro-movements [24–26]. While traditional ergonomic design often relies on static anthropometric data, other design philosophies—such as those influenced by classical Chinese furniture—embrace flexibility and adaptability as key aesthetic and functional elements [27,28].

Thus, the ability of kerfed surfaces to bend in multiple directions enhances both comfort and adaptability, positioning kerf bending as a valuable method for next-generation ergonomic design.

The objective of this study is to investigate the use of laser-cut kerf-bending techniques to create flexible wooden surfaces and to evaluate their applicability in seat design. Specifically, the research focuses on (i) analysing the effects of kerf geometry on flexibility, (ii) optimising kerf patterns, and (iii) assessing the functional and aesthetic performance of the resulting design. This work's

 doi:10.20944/preprints202603.1396.v1

integration of digital fabrication and furniture ergonomics contributes to the growing field of computational design for sustainable and adaptive material applications.

2. Materials and Methods

Based on an understanding of the kerf bending technique and the relevant studies reviewed above, this research links the need for a deeper exploration of a diverse measurement approach. The objective was to compile a comprehensive and systematic table that brings together all kerf patterns currently available, along with the measurement data derived from experimental testing.

The experimental process for the specimens was structured in three consecutive stages. In the first stage, all kerf patterns accessible online were identified, then carefully screened to eliminate any clearly unsuitable examples, and subsequently organised according to the criteria and classifications outlined in the previous chapter. The second stage focused on the fabrication of the selected specimens using a laser cutter. Finally, the third stage involved mechanical evaluation using a universal testing machine and material testing equipment at the Department of Forestry, Wood Sciences, and Design, University of Thessaly, Greece (Figure 1). These tests provided accurate measurements of the specimens' properties. Additional conventional non-destructive testing methods complemented them.

Figure 1. Stages of the experimental process.

2.1. First Stage of Experiments: Pattern Collection

One of the most widely used linear patterns was designed by Aaron Porterfield, consisting of horizontal parallel lines with interruptions at two or three points. This design is valued for its ability to provide both high curvature and strength. As noted in the study by Kalama et al. (2020), modifying the discontinuities in such patterns affects material flexibility: fewer interruptions yield greater curvature but reduced structural strength due to increased material removal.

Alternative variations were created where discontinuities alternated left and right, resulting in highly flexible samples capable of bending up to 180°. Increasing line density enhanced curvature and elasticity but reduced mechanical strength.

In contrast, "wave" and "zigzag" patterns replace straight lines with polygonal, diagonal, or curved chains (Figure 2). This modification disrupts wood fibres at multiple points, thereby maximising curvature capacity.

"Perforated" or "cut-out" patterns, such as "bowling-pin-shaped" perforations, involve complete removal of material in geometric forms, producing transparency and significantly increased flexibility. However, this comes at the cost of reduced structural integrity. These shapes distribute bending forces more evenly, avoiding sharp angles and concentrations of local stress.

"Offset" patterns, composed of shifted triangles, squares, or hexagons, demonstrated high strength and the ability to generate double curvature (Figure 2b). However, points of discontinuity in triangular or square offsets often coincided with fracture locations, while intersections marked zones of maximum curvature. The "honeycomb" pattern, though also involving material removal, was classified as an offset pattern due to its curvature performance depending on the external offset cuts.

The "meander" pattern (Figure 2c), developed by Scott Austin, consists of labyrinth-like continuous lines that combine flexibility and resilience. Variations demonstrated that smaller-scale

 doi:10.20944/preprints202603.1396.v1

meanders increased flexibility but decreased strength. Parametric modifications of meanders, including rounded corners or triangular/hexagonal adaptations, generated new behaviours ranging from single to double curvature.

Finally, "parametric" patterns (Figure 2d) were developed using algorithmic design, incorporating adjustable parameters such as line density, spacing, length, orientation, and discontinuity. These produced complex double-curvature behaviours, with densification at specimen centres enabling maximum curvature.

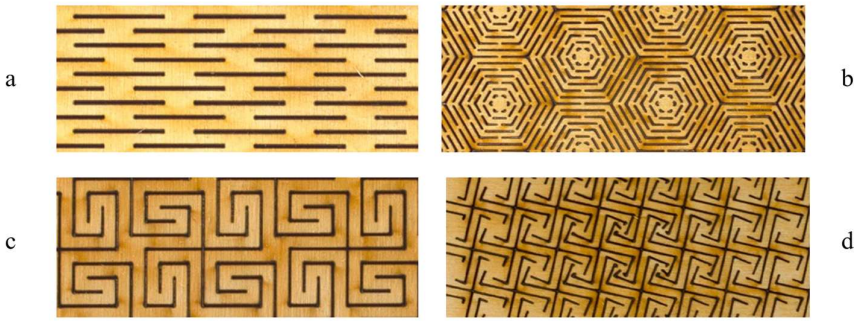

Figure 2. Linear patterns of parallel lines: a) Linear patterns of parallel lines, b) Offset patterns, c) Meander patterns, "Greek-key patterns", d) Parametric patterns.

The first experimental stage concluded with the final selection of 56 unique patterns, including original designs and their variations.

The patterns were collected following extensive online research, as the kerf-bending technique with laser cutting primarily relies on digital files for fabrication. This reliance on digital resources makes it challenging to find such patterns within conventional bibliographic references.

During the collection process, several widely used designs were identified, including parallel line patterns and meander-type patterns. However, some patterns that were initially presented as suitable proved incompatible as their cutting would have segmented the piece completely, eliminating structural cohesion and thereby preventing curvature. In certain cases, this limitation was not immediately apparent; for instance, some sample files failed to bend when cut at their original scale, requiring further modification.

To process the collected patterns and prepare them for final cutting, the software "Rhinoceros" and "AutoCAD" were employed. Using both software, variations of existing patterns were created by adjusting scale, line spacing, and line morphology (e.g., replacing sharp corners with filleted curves), as well as by altering density (parametric density variations). Through this process, new patterns with distinct bending capabilities were generated.

Patterns were initially divided into two major categories: those enabling single curvature and those capable of double curvature. A more detailed classification was then developed, combining both previously established typologies and newly observed or designed patterns. The final categorisation is as follows (with corresponding numbering as listed below (Table 1):

Table 1. Design pattern categorisation.

Type of pattern	Pattern numbers
Linear (parallel lines)	1–5
Wave or zigzag	6–11
Perforated / cut-out (closed shapes with material removal)	12–26.2
Offset	27–34
Meander	35–41.2
Parametric	42–42.3

 doi:10.20944/preprints202603.1396.v1

2.2. Second Stage of Experiments: Pattern Cutting

Following the collection and preparation of the digital designs, the second stage involved the fabrication of test specimens using a 150 W CO_2 laser cutting CNC machine. The cutting parameters were set to 70 - 30 (Power: W - Laser speed: mm/s), with a laser beam width of 0.15 mm (Figure 3).

The primary material selected was birch plywood, first with a thickness of 3 mm, followed by 4 mm, to enable comparative evaluation of bending properties. The specimens were cut into standardised dimensions for consistency across tests. Natural defects such as knots, voids, or seams, as well as variations in adhesive layers, were noted as potential sources of structural irregularities.

Cutting times were recorded for each specimen and are summarised in the consolidated table, ranging from 1 to 9 minutes, depending on the pattern lines' density.

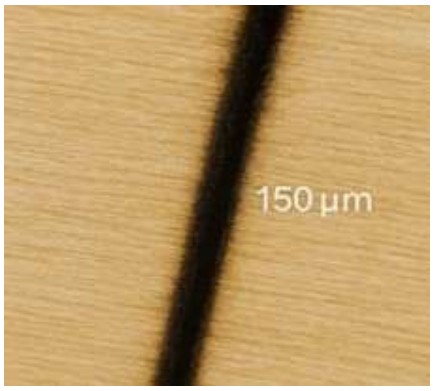

Figure 3. Laser beam width using an optical zoom device.

During initial cutting trials, several errors were observed. Some collected patterns, due to scale or dimensional issues, produced excessively rigid specimens. This necessitated a second round of design modifications. Additional issues arose from inherent material defects such as knots, seams, voids, or variations in adhesive layers, which occasionally caused localised cutting failures and required reprocessing.

In total, 112 specimens were fabricated: 56 from 3 mm birch plywood and 56 from 4 mm birch plywood. For the supplementary bending angle experiment (a non-destructive method measuring the degree of curvature in single-bend specimens), an additional 56 specimens were cut with extended material tabs on one side to allow secure clamping. These later served as reference samples for the final catalogue presentation.

2.3. Third Stage of Experiments: Measurement Methods

2.3.1. Mechanical Testing (Destructive)

After specimen fabrication, the third and final stage involved evaluating mechanical and bending properties using both conventional and advanced measurement methods. The material used was an industrial wood-based panel characterised by high mechanical performance, with a moisture content of 12% and an average density of 0.70 g/cm³ (700 kg/m³). The bonding of the individual veneer layers was achieved using phenolic resin adhesive of the WBP type (Water Boiled Proof), which provides enhanced resistance to moisture and outdoor environmental conditions. The original industrial panels' dimensions were 2500 × 1250 mm, from which the specimens used in the experimental procedure were produced. In terms of mechanical properties, the initial modulus of elasticity in bending (E) of the solid material without processing is estimated to be approximately 8000 N/mm² (≈ 8000 MPa) for the 3 mm thickness and approximately 9000 N/mm² (≈ 9000 MPa) for the 4 mm thickness. These values fall within the typical range for high-quality birch plywood and are used as the baseline mechanical reference for comparing the behaviour of the specimens after the application of the kerf bending technique.

 doi:10.20944/preprints202603.1396.v1

The evaluation of the mechanical properties of the specimens was conducted in accordance with the European standard EN 310, which is widely used for determining the bending strength and the modulus of elasticity in bending (E) of wood-based panels through a three-point bending test. In this test, the specimen is supported at two points and loaded vertically at the midpoint of the span until failure occurs. The maximum load recorded during the test (Fmax) is expressed in Newton (N) and is used to calculate the bending strength, which is expressed as stress in Megapascal (MPa), where 1 MPa = 1 N/mm². Additionally, the slope of the load–displacement curve within the elastic region is used to determine the corresponding modulus of elasticity. The standard has been developed for solid and structurally homogeneous panels, in which the cross-section remains continuous. The mechanical response can be approximated as the bending behaviour of a single beam with a relatively uniform stress distribution. The EN310 standard stipulates that the samples have two support points. The double curvature of the Kerf was used to highlight the samples' properties by creating four support points in a square frame using the specimens coming from flat sheets.

The primary method, a core objective of this study, involved measuring the fracture point and modulus of elasticity of the 112 specimens using a Zwick/Roell Z020 universal testing machine (Figure 4).

Figure 4. Zwick/Roell Z020 Universal testing machine.

A custom wooden frame (150 × 150 mm) was constructed to hold specimens at four points, simulating a seating frame. A plunger was used to apply force to the specimen centre until it failed, while also recording load values in Newtons (N) and creating stress-strain graphs (Figure 5). This approach was particularly suitable for double-curvature patterns, though single-curvature specimens were also measured to provide a complete dataset. Due to specimen fracture during testing, these samples could not be reused.

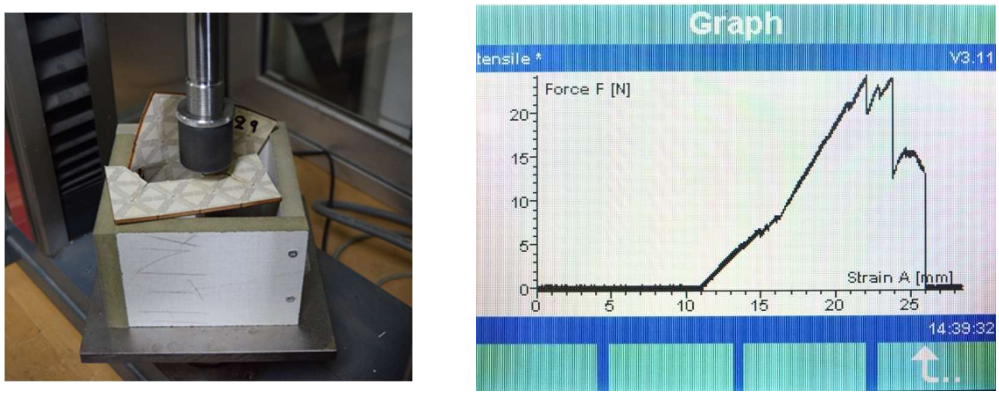

(**a**) (**b**)

Figure 5. Zwick/Roell Z020 Fracture of specimen No. 29 (a) and the corresponding graph (b).

 doi:10.20944/preprints202603.1396.v1

2.3.2. Conventional Testing (Non-Destructive)

In addition to destructive testing, a non-destructive bending angle method was employed. This method focuses on (i) measuring the bending angle of specimens (in degrees) under single curvature, (ii) applying loads with weights on single-curvature patterns, allowing for comparison of flexibility across patterns without compromising structural integrity, and (iii) assessing double-curvature patterns by applying localised force.

The angle measurement experiment was particularly suitable for specimens with single curvature and was also performed on all double-curvature patterns to investigate whether these designs could function along a single axis. For this test, a custom protractor was designed and mounted onto a vertical base, enabling the specimens to be clamped securely on one side (Appendix: Table A1). The free side was then allowed to bend along one axis, and the resulting angle was recorded using the protractor.

In the weight-loading experiment, specimens were fixed along two edges, allowing bending exclusively along a single axis (single curvature). Weights were applied incrementally until the specimens approached their fracture threshold. For double-curvature patterns, the method was modified: the four corners of the specimen were supported on independent bases, leaving them free, while force was applied at the centre. This configuration allowed the surface to form a convex double curvature.

Some specimens elongated during this process, while others did not approach fracture even under maximum applied load. In total, up to four weights of 200 g each (maximum load: 800 g) were applied to certain single-curvature specimens. For other cases, manual surface pressure was applied until resistance was encountered during bending (Appendix: Table A2). The combined results from both destructive and non-destructive tests were consolidated into a comparative database, enabling systematic evaluation and selection of the most suitable kerf patterns for subsequent application in the seating prototype.

Patterns were organised into a digital library of 56 designs, categorised by curvature type and geometry. Visual inspection of kerf patterns focused on curvature smoothness, absence of cracks, and reduction of burn marks from laser cutting.

The combined results from destructive and non-destructive methods allowed the creation of a comprehensive database of kerf pattern performance, used to select the most suitable designs for the seating prototype.

2.4. Kerf Patterns

Based on an extensive collection, modification, and classification process, 56 kerf patterns were selected and tested. These patterns were grouped into six main categories:

The first category was the “linear” patterns (1–5). Parallel straight cuts, including widely used designs such as Aaron Porterfield’s interrupted-line pattern, are capable of bending up to 180° with variations in density and discontinuities. These provide high curvature but reduced strength as kerf density increases.

The second category was the “wave/zigzag” patterns (6–11). These patterns are derived from linear patterns by replacing straight cuts with diagonal, polygonal, or wavy lines. They disrupt fibres in multiple directions, enhancing flexibility and enabling greater curvature.

The third category was “perforated/cut-out” patterns (12–26.2). They consist of geometric cut-outs (e.g., bowling pin shapes) that fully remove material. These result in transparency and uniform elasticity but reduce overall structural integrity.

The fourth category was the “offset” patterns (27–34). They are formed by shifted shapes (triangles, squares, hexagons), including honeycomb structures. These designs provide high strength and can achieve double curvature, though stress points often appear at discontinuities.

The fifth category was the “meander” patterns (35–41.2). A labyrinth-like continuous line design (Scott Austin’s model) is valued for its balance of flexibility and resilience. Smaller-scale

 doi:10.20944/preprints202603.1396.v1

meanders increase curvature but reduce strength. Variations with rounded corners, triangles, and hexagons expand their performance from single to double curvature.

The sixth category was the "parametric" patterns (42–42.3). Those were generated through algorithmic design, with adjustable variables such as line density, spacing, and curvature direction. These patterns concentrate flexibility in specific regions (often at the centre), enabling double curvature and highly controlled bending performance.

3. Results

Following the acquisition of all necessary measurements with the universal testing machine, the results were compiled in a consolidated table (Annex: Table 2) and further analysed comparatively. The analysis examined values across patterns and material thicknesses, while the relationship between kerf geometry, percentage of material removal, and their combined influence on curvature and mechanical strength was reviewed. Special emphasis was given to double-curvature patterns to identify indicative applications for each and select the most suitable candidates for subsequent application (in a flexible seating prototype).

Table 2. Potential application groups for "double curvature" patterns based on the Fmax.

Application groups	Pattern numbers
Decorative and visual applications	27, 28, 41
Interior cladding and surface coverings	29, 34, 36, 39, 41.1, 41.2
Load-bearing surfaces (e.g., seats and backrests)	30, 31, 32, 38, 42, 42.2
Curved cladding or backrest panels	33, 35, 37, 40, 42.1, 42.3

3.1. Comparison of Fmax Values by Thickness

From the comparative analysis of Fmax (N) values for all patterns at the two tested thicknesses (3 mm and 4 mm), it was observed that the 3 mm specimens consistently achieved higher Fmax values than their 4 mm counterparts. The thinner plywood offered better deformation capacity before fracture and more efficient distribution of internal stresses.

Specifically, patterns No. 30, 32, 38, and 42.2 at 3 mm thickness exhibited significantly high Fmax values, maintaining stable curvature and thus proving ideal for applications requiring a balance of strength and elasticity (Annex: Table 3). In contrast, patterns such as No. 27 and No. 41 recorded particularly low Fmax values, rendering them suitable only for non-structural or decorative uses. A bar chart was produced to visualise Fmax values per thickness and collectively across all patterns (Figure 6).

Table 3. Descriptive statistical analysis (Fmax), using SPSS software.

Statistics	4 mm (N)	3 mm (N)
Mean	172.16	211.16
Standard deviation	138.27	175.15
Minimum	19.10	26.80
Median	138.53	145.16
Maximum	587.47	765.61

 doi:10.20944/preprints202603.1396.v1

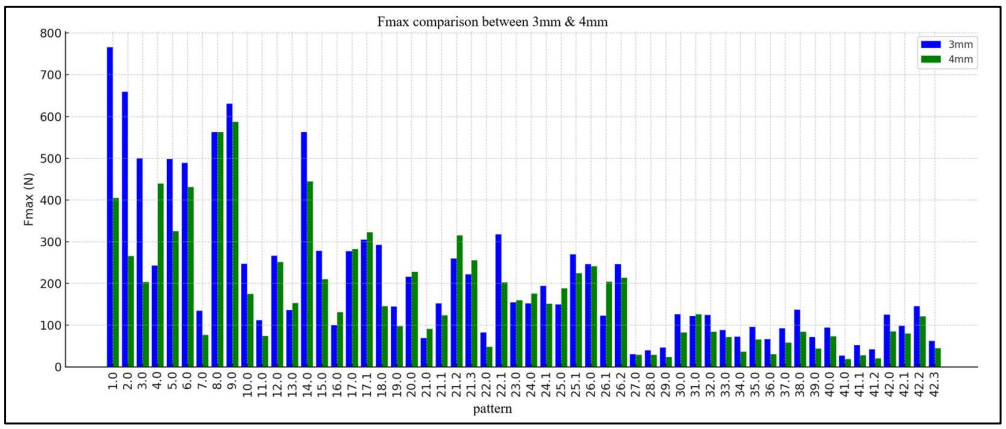

Figure 6. Consolidated bar chart of Fmax (N) values for all kerf patterns by material thickness.

3.2. Influence of Material Removal Percentage

Analysis of the percentage of material removed (as calculated per pattern and reported in the consolidated Table 3) revealed notable variations in how geometry impacts mechanical and ergonomic behaviour. Percentages ranged from approximately 3% to nearly 60%, offering a wide diversity of kerfing approaches (Figure 7).

However, the ratio of removed to retained material was not always a strict determinant of flexibility. Certain geometries with low removal percentages (e.g., "parametric" patterns) achieved high deformation due to efficient structural distribution, while others with high removal percentages demonstrated reduced strength because of diminished cross-sectional resistance to stress. These results highlight the importance of geometry over raw material removal.

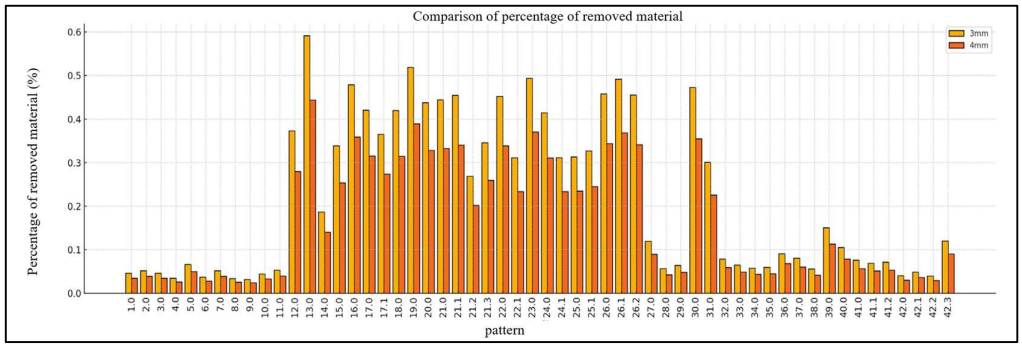

Figure 7. Consolidated bar chart of material removal percentages per pattern.

3.3. Performance of Double-Curvature Patterns

For double-curvature patterns (No. 27–42.3), force–deformation diagrams obtained from the mechanical performance tests indicated that several designs achieved high Fmax values along with favourable elastic–plastic behaviour. Once again, 3 mm specimens outperformed 4 mm specimens, combining larger bending capacity with higher peak loads (Figure 8). Patterns No. 32, 35, 38, 40, 42, 42.1, 42.2, and 42.3 showed the best overall mechanical behaviour.

 doi:10.20944/preprints202603.1396.v1

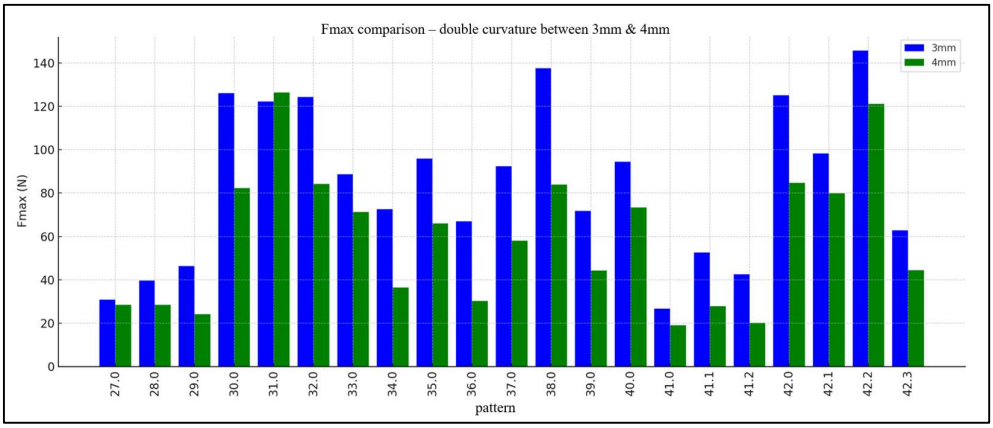

Figure 8. Bar chart of Fmax (N) values for double-curvature kerf patterns.

3.4. Indicative Applications of Double-Curvature Patterns

Based on their Fmax values, "double curvature" patterns were categorised into four indicative application groups (Table 2). From this classification, the most suitable candidates for seating applications were determined as those combining progressive deformation, high Fmax values, and the ability to generate double curvature. These included patterns No. 32, 35, 38, 40, 42, 42.1, 42.2, and 42.3.

Notably, patterns No. 42 and 42.2 exceeded 125 N Fmax at 3 mm thickness, allowing smooth loading without permanent deformation. Patterns No. 38 and 40 demonstrated gradual force increases with steady curvature. Although pattern No. 42.3 did not record the highest Fmax, it exhibited strong elasticity and recovery capacity, making it valuable for ergonomic surfaces.

The analysis confirmed that geometry plays a more decisive role than thickness or removal percentage in determining kerf-bent performance.

The experimental results confirmed that kerf geometry plays a decisive role in determining the flexibility of plywood panels. Linear kerfs with dense spacing (≈3 mm) achieved a bending radius as low as 50 mm, enabling significant curvature. By contrast, wider spacings (> 6 mm) reduced flexibility and restricted the bending angle. "Wave" and "zigzag" patterns offered higher adaptability, as the angled or sinusoidal kerfs disrupted fibres along multiple directions. "Parametric" designs concentrate curvature in specific regions, allowing controlled deformation and, in some cases, achieving double curvature, which is not possible with traditional linear cuts. Generally, thinner specimens (3 mm plywood) consistently exhibited greater curvature than 4 mm specimens, demonstrating that thickness reduction enhances flexibility without catastrophic loss of stability.

Mechanical testing with the Zwick/Roell Z020 revealed that while kerf bending inevitably reduces the load-bearing capacity of the birch plywood, certain patterns maintained 60–70% of the original strength. Patterns with balanced material removal, such as offset or meander designs, exhibited the best trade-off between flexibility and strength.

The maximum force values (Fmax) for 3 mm specimens were generally higher than those of 4 mm specimens, as the thinner panels distributed stresses more effectively under bending. Notably, patterns No. 32, 35, 38, 40, 42, 42.1, 42.2, and 42.3 combined high Fmax values with progressive, non-brittle failure modes, making them strong candidates for structural furniture applications. Patterns with excessive material removal (up to 60%) exposed reduced mechanical resistance, confirming that while flexibility increases, the cross-section resistance is diminished. Conversely, "parametric" geometries demonstrated that efficient kerf arrangements can achieve satisfactory strength even at relatively low removal percentages.

In addition to mechanical performance, the kerf patterns were evaluated for their visual and tactile qualities. Excessive burn marks were minimised by adjusting laser settings (lower power and higher cutting speed), resulting in clean kerfs with smooth edges. From a design perspective, "linear"

 doi:10.20944/preprints202603.1396.v1

and "parametric" patterns provided the most visually seamless transitions, producing organic and flowing surfaces that enhanced the aesthetic quality of the bent panels. "Perforated cut-out" designs added transparency and visual lightness, although their reduced strength limited their functional applications. The evaluation confirmed that kerf patterns not only modify the mechanical properties of wood but also act as decorative design elements, contributing to both functional and aesthetic qualities in furniture applications.

3.5. Statistical Analysis.

IBM's SPSS Statistics software was used to process and analyse experimental data. A descriptive statistical analysis of the maximum bending strength values (Fmax) was performed, calculating the mean, standard deviation, median, minimum and maximum values for the 3 mm and 4 mm thick specimens (Table 3). Using the Shapiro-Wilk and Kolmogorov-Smirnov tests, the normality of the data was assessed. Since the data were not normally distributed (Tables 4 and 5), the nonparametric Mann-Whitney U test was used to compare the two groups (Table 4). For completeness, a parametric t-test of independent samples was also performed with Welch's correction. Relative variability of the results was assessed using the coefficient of variation (CV), while the magnitude of the effect of thickness was estimated using Cliff's delta, which is suitable for nonparametric data. Lastly, a two-parameter Weibull analysis was applied to evaluate the reliability and the fracture behaviour of the specimens. In all statistics, the level of statistical significance was set at 0.05. Both datasets significantly deviate from normality ($p < 0.05$).

Table 4. The Shapiro-Wilk normality test.

Variable	W statistic	p-value	Normality
Fmax / 4 mm	0.880	$p < 0.001$	Not normal
Fmax / 3 mm	0.821	$p < 0.001$	Not normal

Table 5. The Kolmogorov–Smirnov normality test.

Variable	D statistic	p-value	Normality
Fmax / 4 mm	0.134	0.243	Cannot reject normality
Fmax / 3 mm	0.215	0.009	Not normal

The Kolmogorov–Smirnov test demonstrated that the 3 mm specimens' data clearly violate normality, and the 4 mm specimens' results are mixed; hence, the Shapiro–Wilk is considered more reliable. The Shapiro–Wilk test indicated that Fmax datasets deviate significantly from normality ($p < 0.001$). Therefore, a non-parametric Mann–Whitney U test was used to compare the maximum force between 3 mm and 4 mm specimens.

The analysis revealed no statistically significant difference between the two thicknesses ($U = 1355$, $p = 0.216$). Parametric t-test results led to the same conclusion ($p = 0.194$) but were considered secondary due to violation of normality assumptions.

To undertake a comparison between 3 mm and 4 mm specimens, a parametric test was also undertaken: Independent samples t-test (Welch)

H_0: Mean (Fmax 3 mm) = Mean (Fmax 4 mm)

$t = -1.31$ $p = 0.194$

No statistically significant difference between means ($\alpha = 0.05$). The non-parametric test: Mann–Whitney U test, makes the hypothesis:

H_0: The distributions of Fmax are equal

$U = 1355$ $p = 0.216$

 doi:10.20944/preprints202603.1396.v1

The test showed no statistically significant difference between 3 mm and 4 mm (α = 0.05). In conclusion, both distributions were strongly right-skewed, with the majority of values concentrated below approximately 250 N for the 4 mm specimens and below 300 N for the 3 mm specimens, while several high-force outliers exceeded 500 N. This behaviour suggested that the data were unlikely to follow a normal distribution.

Normality was assessed using the Shapiro–Wilk test, which indicated significant deviation from normality for both thicknesses ($p < 0.001$). Although the Kolmogorov–Smirnov test produced mixed results—failing to reject normality for the 4 mm specimens but rejecting it for the 3 mm specimens—the Shapiro–Wilk test was considered more reliable for the given sample size. Consequently, both datasets were treated as non-normally distributed. Given the violation of normality assumptions, a non-parametric Mann–Whitney U test was employed to compare the Fmax values between thicknesses (Figure 9). The test revealed no statistically significant difference between the 3 mm and 4 mm specimens ($U = 1355$, $p = 0.216$). For completeness, a Welch independent-samples t-test was also performed and yielded a consistent result ($t = -1.31$, $p = 0.194$), although it was considered secondary due to the lack of normality.

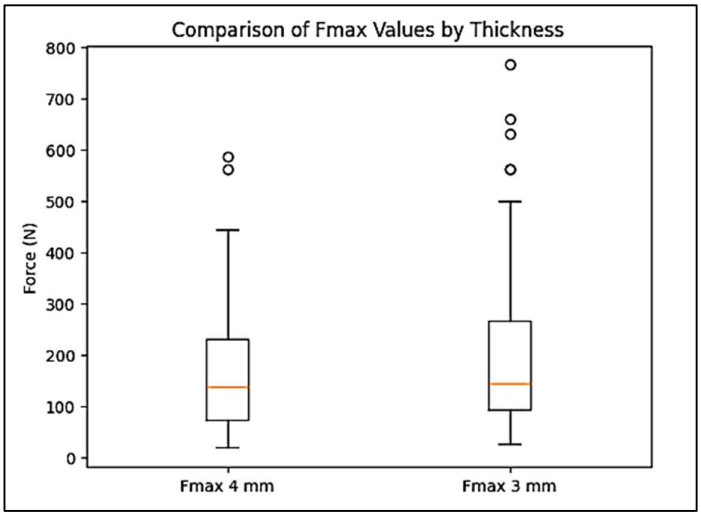

Figure 9. Comparison of Fmax (by thickness).

The coefficient of variation (CV) was calculated to assess relative variability and reliability (Table 6). The coefficient of variation quantifies relative variability and is crucial for reliability assessment. Both thicknesses exhibited extremely high CV values, exceeding 80%, which indicates substantial scatter and low repeatability. The 3 mm specimens showed slightly higher variability, suggesting marginally lower consistency despite their higher mean strength. This high scatter explains why numerical differences in mean Fmax did not translate into statistically significant results.

Table 6. Coefficient of Variation (CV %).

Thickness	Mean Fmax (N)	Std. Dev. (N)	CV (%)
4 mm	172.16	138.27	80.3
3 mm	211.16	175.15	82.9

Because normality is violated, Cliff's delta is the correct effect size. Cliff's $\delta = 0.136$, which shows a negligible practical effect. Although the 3 mm specimens exhibited a higher mean maximum force compared to the 4 mm specimens, both datasets showed extremely high coefficients of variation (> 80%), indicating significant scatter and low repeatability.

 doi:10.20944/preprints202603.1396.v1

A Mann–Whitney U test revealed no statistically significant difference between thicknesses ($p = 0.216$), and the effect size measured by Cliff's delta ($\delta = 0.136$) was negligible. These results suggest that thickness alone does not govern bending strength, and failure behaviour is dominated by material variability and defect sensitivity rather than nominal geometry. A two-parameter Weibull distribution was fitted to the maximum force (Fmax) data for both specimen thicknesses (3 mm and 4 mm), assuming a zero-threshold load. Weibull reliability analysis revealed that both 3 mm and 4 mm specimens exhibit low Weibull modulus ($\beta \approx 1.3$), indicating highly scattered, defect-controlled failure behaviour (Figure 10, Table 7). Although the 3 mm specimens demonstrated a higher characteristic strength ($\eta = 231$ N) compared to the 4 mm specimens ($\eta = 187$ N), the similarity of Weibull moduli and the strong overlap of reliability curves indicate comparable reliability levels. Consequently, the observed increase in mean strength for thinner specimens does not translate into a statistically or practically significant reliability improvement.

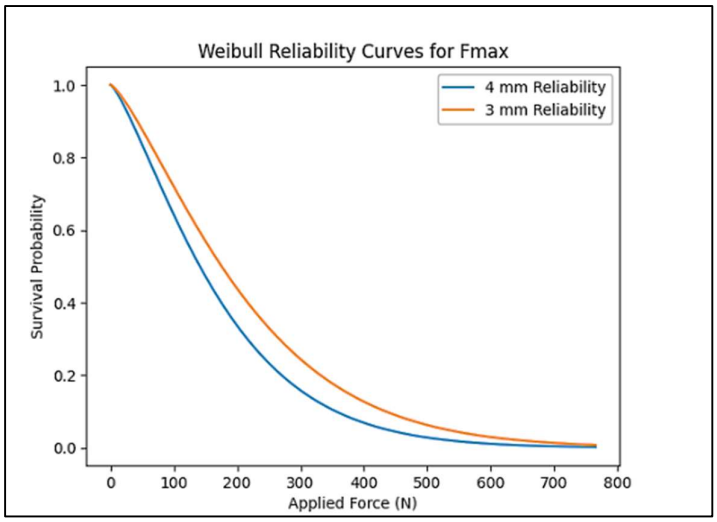

Figure 10. Weibull reliability curves for Fmax.

Table 7. Weibull reliability analysis.

Thickness	Shape β (Weibull modulus)	Scale η (N)	Interpretation
4 mm	1.3	187	Lower characteristic strength
3 mm	1.32	231	Higher characteristic strength

4. Discussion

In the present study, the specimens were processed using the kerf bending technique, which involves the introduction of a series of repeated cuts into the material to increase flexibility and enable the formation of curved surfaces. This process results in partial material removal and consequently reduces the effective cross-sectional area and the overall stiffness of the specimen, while simultaneously creating regions of stress concentration between the cuts. As a result, the deformation of the specimens does not arise solely from elastic bending but rather from a combination of bending, localised rotations, and the gradual opening of the kerfs. For this reason, the mechanical response deviates to some extent from the theoretical model of a continuous beam. Despite these differences, the three-point bending test provides a reliable and comparable framework for the comparative evaluation of different kerf bending geometrical patterns. The analysis of the load–displacement curves recorded by the Zwick Roell Z020 testing system enabled the assessment of the elastic response, stiffness, and deformation capacity of the specimens, while the maximum failure load

 doi:10.20944/preprints202603.1396.v1

(Fmax) was used as the primary indicator of mechanical performance for comparing the different patterns.

The selection of two different material thicknesses (3 mm and 4 mm) allowed the investigation of the influence of thickness on both the structural strength and the bending capability of the kerf bending patterns. Increasing the thickness directly affects the stiffness of the cross-section and consequently the load-bearing capacity of the specimen, while simultaneously reducing the maximum achievable deformation before failure. Through the comparative analysis of Fmax values, load–displacement curves, and the overall failure behaviour of the specimens, it becomes possible to examine the relationship between pattern geometry, material thickness, and mechanical performance, providing a reliable framework for evaluating the suitability of kerf bending patterns for applications involving curved wooden structures.

The findings of this study confirm that kerf geometry is the most critical factor influencing the mechanical and ergonomic behaviour of birch plywood panels subjected to laser cutting. While thickness and percentage of material removal also play significant roles, the efficiency of the geometric arrangement often outweighs these variables.

5. Conclusion and Future Steps

This research has shown that the technique of kerf bending using a laser cutting CNC machine is a viable and sustainable technique for producing flexible wooden surfaces, enabling single and double curvature without the need for steam bending or lamination. Geometry dominates performance: “parametric” and “meander” patterns, particularly design numbers: 32, 35, 38, 40, 42, 42.1, 42.2, and 42.3, achieved the best combination of high curvature capacity, gradual deformation, and load resistance. Moreover, thinner plywood (3 mm) consistently outperformed the 4 mm sheets in terms of flexibility and Fmax but requires reinforcement in practical applications. The material removal percentage alone is not predictive of flexibility or strength; efficient geometries can achieve high performance even at lower removal ratios.

As for aesthetic value, it is an intrinsic outcome of kerf bending: the cut patterns function as both structural solutions and expressive visual elements. In conclusion, kerf bending merges digital precision, ergonomic adaptability, and aesthetic expression, reinforcing its potential as a technique for contemporary furniture and architectural applications.

While this study provides a comprehensive balance, several areas require further exploration. Future studies should investigate kerf bending in alternative wood species, engineered panels, and even bio-based composites to broaden the applicability of this technique.

Another area of investigation refers to the performance of kerf-bent panels under cyclical loading, humidity changes, and wear, which should be evaluated to determine their reliability in daily use. Parametric and algorithmic design approaches could be developed further, enabling automated generation of kerf geometries optimised for specific curvature and load conditions. In addition, combining kerf bending with lamination, fabric backings, or embedded composites could enhance strength without compromising flexibility. While this work demonstrated application at the furniture scale, larger prototypes such as partitions, wall panels, or architectural surfaces could demonstrate kerf bending’s potential in spatial design. Future prototypes could integrate user testing to evaluate comfort, adaptability, and perception of kerf-bent surfaces in real-world use.

Supplementary Materials: The following supporting information can be downloaded at the website of this paper posted on Preprints.org, Catalogue and Photographic Material of Specimens, Kerf Bending Patterns - Summary Table.

Author Contributions: For research articles with several authors, a short paragraph specifying their individual contributions must be provided. The following statements should be used “Conceptualization, E.G. and G.N.; methodology, G.N.; software, E.G.; validation, E.G, G.N. and K.N.; formal analysis, E.G.; investigation, E.G; resources, E.G.; data curation, K.N.; writing—original draft preparation, K.N.; writing—review and editing,

 doi:10.20944/preprints202603.1396.v1

K.N.; visualization, E.G.; supervision, G.N; project administration, K.N.; All authors have read and agreed to the published version of the manuscript.

Funding: This research received no external funding.

Institutional Review Board Statement: Not applicable.

Conflicts of Interest: The authors declare no conflicts of interest.

References

1. Smith, J., & Taylor, K. Traditional wood bending techniques: A comparative study. Wood Science and Technology, 2018. 52(5), pp. 1123–1135.
2. Anderson, R., & Peters, J. Digital fabrication in furniture design: Opportunities and challenges. Journal of Design and Technology, 2017. 12(3), pp. 145–159.
3. Müller, T., Reiter, F., & Schmidt, H. Parametric kerfing: Controlling flexibility in plywood structures. Proceedings of the International Conference on Digital Fabrication, 2015. pp. 102–110.
4. Singh, A., & Gupta, P. Effects of kerf geometry on mechanical flexibility of wood composites. Materials Today: Proceedings, 2020. 28, pp. 233–240.
5. Egorov, V., Andersen, H., & Peters, J. Advanced kerf structures in architectural design. [Conference presentation]. 2023.
6. Zhao, L., & Li, Y. Laser cutting and kerf bending for adaptive structures. Journal of Manufacturing Processes, 2019. 37, pp. 210–219.
7. Darnal, A., Poluri, K., Deshpande, H., Kim, J., Kalantar, N., & Muliana, A. An exploration of 3D-printed freeform kerf structures. Behavior and Mechanics of Multifunctional Materials XVII, 12. 2023. https://doi.org/10.1117/12.2658554
8. Condoroteanu, C.D., Gurau, L., Cosereanu, C., Georgesku, S.V. Proposed method to evaluate the effect of changing the kerfing parameters upon the static bending behavior of flexible plywood panels cut by laser. Appl. Sci. 2022, 12(9), 4303; https://doi.org/10.3390/app12094303
9. Gautam, G. D., & Mishra, D. Multiple kerf quality optimization in laser cutting of BFRP composite using grey relational-based genetic algorithm. FME Transactions, 2022. 48(3), pp. 636–650. https://doi.org/10.5937/fme2003636g
10. Eltawahni, H. A., Rossini, N., Dassisti, M., Alrashed, K., Aldaham, T., Benyounis, K., & Olabi, A. G. (2013). Evaluation and optimization of laser cutting parameters for plywood materials. Optics and Lasers in Engineering, 51(9), 1029–1043. https://doi.org/10.1016/j.optlaseng.2013.02.019
11. Kechagias, J.D., Ninikas, K., Salonitis, K. An experimental study of laser cutting of PLA-wood flour 3D printed plates using a modified Taguchi design. Int. J. Experimental Design and Process Optimisation, Vol. 7, No. 1, 2022. pp. 62–75.DOI: 10.1504/IJEDPO.2022.131230
12. Kechagias J.D., Ninikas K., Stavropoulos P., Salonitis K. A Generalised Approach on Kerf Geometry Prediction during CO2 Laser cut of PMMA Thin Plates using Neural Networks. "Journal of Lasers in Manufacturing and Materials Processing". Springer. 2021. DOI:10.1007/s40516-021-00152-4
13. Kolarevic, B.Architecture in the digital age: Design and manufacturing. Spon Press. 2003.
14. Oxman, N. Material ecology. Computational Design Journal, 6(1), 2012. pp. 12–21.
15. Helander, M. A guide to human factors and ergonomics. CRC Press. 2003.
16. Lange, M., & Albers, A. Flexible structures through kerf cutting: Applications in product design. Design Research Journal, 9(2), 2016, pp. 33–42.
17. Darnal, A., Mantri, K., Farajmandi, A., Kalantar, N., Azari, E. R., & Muliana, A. Additively manufactured kerf structures: Flexibility, energy absorption, and load-bearing behaviors. International Journal of Solids and Structures, 314, 2025, 113331.
18. Cheng, L. Y., Ferreira, S. L., & Pereira, L. Kerf bending–An experimental study on the design parameters. In International Conference on Geometry and Graphics 2024, pp. 352–363. Springer Nature Switzerland.
19. Maalej, E.Developing the MLJ: A variable and scalable alternative to conventional bent wood lamination formworks. The Pennsylvania State University. 2025.

 doi:10.20944/preprints202603.1396.v1

20. Lorenzoni, B. R., & Silva, F. P. D. Geometric analysis of the MDF kerf-bending structure accuracy. International Journal of Space Structures, 37(2), 2022, pp. 135–149.
21. Chenrayan, V., Manivannan, C., Shahapurkar, K., Zewdu, G. A., Maniselvam, N., Alarifi, I. M., ... & Algahtani, A. An experimental and empirical assessment of machining damage of hybrid glass-carbon FRP composite during abrasive water jet machining. Journal of Materials Research and Technology, 19, 2022, pp. 1148–1161.
22. Trajković, A., & Madić, M. Analysis and optimization of kerf width in fiber laser cutting of S235 steel. Jordan Journal of Mechanical and Industrial Engineering, 2024, 18(3).
23. Shahnewaz, M., Jackson, R., & Tannert, T. LT concrete composite floors with steel kerf plate connectors. Construction and Building Materials, 339, 2022, 127678.
24. Shahid, Z., Hubbard Jr, J. E., Kalantar, N., & Muliana, A. An investigation of the dynamic response of architectural kerf structures. Acta Mechanica, 233(5), 2022, pp. 2189–2210.
25. Bhooshan, V., Louth, H. D., & Bhooshan, S. Democratising tectonism: High performance geometry for mass-customisation of virtual and physical spaces. In Disruptive Technologies: The Convergence of New Paradigms in Architecture, Springer International Publishing, 2023, pp. 167–190.
26. Donkoh, M. B. Assessment of occupational health and safety of wood machining operation at a wood processing and marketing centre in Ghana. University of Education, Winneba. https://uew.edu.gh, 2021.
27. Chen, R. Attaining desired deformations of flexible structures through mechanical and non-mechanical stimuli. 2019, [PDF].
28. Saslawsky, K., Steixner, C., Tucker, M., Costalonga, V., & Dahy, H. FlaxPack: Tailored natural fiber reinforced (NFRP) compliant folding corrugation for reversibly deployable bending-active curved structures. Frontiers in Materials Science. 2024.